

# Limits on sizes of fundamental particles and on gravitational mass of a scalar

Irina Dymnikova<sup>1</sup>, Jürgen Übrig<sup>2</sup> and Jiawei Zhao<sup>3</sup>

<sup>1</sup>Institute of Mathematics and Informatics, UW M in Olsztyn, PL 10-561 Olsztyn, Poland  
<sup>2</sup>Labor für Hochenergiephysik, ETH-Hönggerberg, HPK 40, CH-8093 Zurich, Switzerland  
<sup>3</sup>Chinese University of Science and Technology, USTC, Anhui 230029 Hefei, P.R. China

**Abstract.** We review the experimental limits on mass of excited fundamental particles and contact interaction energy scale parameters for QCD, QED and electroweak reactions. In particular we have focused on the QED reaction measuring the differential cross-sections for the process  $e^+ e^- \rightarrow \gamma \gamma$  at the energies from 91 GeV to 202 GeV using the data collected with the L3 detector from 1991 to 1999. With a global fit we set lower limits at 95% CL on  $m > 1687$  GeV, which restricts the characteristic QED size of the interaction region to  $R_e < 1.7 \times 10^{-17}$  cm. All the interaction regions are found to be smaller than the Compton wavelength of the fundamental particles. This constraint is used to estimate a lower limit on the size of a fundamental particle related to gravitational interaction, applying the model of self-gravitating particle-like structure with the de Sitter vacuum core. It gives  $r < 2.3 \times 10^{-17}$  cm and  $r_e < 1.5 \times 10^{-18}$  cm, if leptons get masses at the electroweak scale, and  $r < 3.3 \times 10^{-27}$  cm,  $r_e < 4.9 \times 10^{-26}$  cm, as the most stringent limits required by causality arguments. This sets also an upper limit on the gravitational mass of a scalar  $m_{scalar} < 154$  GeV at the electroweak scale and  $m_{scalar} < 3.8 m_{Pl}$  as the most stringent limit.

## INTRODUCTION

In recent years, three experimental approaches have been developed to test the size of fundamental particles (FP). First, a search is performed for excited states of FP and a corresponding mass is estimated [1]. Second, a characteristic scale parameter is determined, constraining a characteristic size of the interaction region for the reaction [1]. Third, a form factor  $R$  [2] has been used to estimate the sizes of FP.

None of the measurements of the mass of excited FP, and  $R$  show a signal in frames of QCD, QED and electroweak theory, but it was possible to set stringent limits on all parameters. In this paper we present, first, new experimental limits in the QED part and prove that all the limits, set by QCD, QED and electroweak interaction on the characteristic sizes of the interaction region and form factors, are smaller than the Compton wavelengths  $\lambda_c = \hbar/mc$  of FP. Second, we assume that

whatever would be a mechanism of a mass generation, a FP must have an internal core related to its mass and a finite geometrical size defined by gravity. To estimate it we apply de Sitter-Schwarzschild geometry which is the analytic globally regular modification of the Schwarzschild geometry corresponding to replacing a singularity with a de Sitter vacuum core. This allows us to estimate an upper limit on a self-coupling and on the gravitational mass of a scalar, and to set the lower limits on sizes of FP as related to gravitational interaction ([3] and references therein).

## EXPERIMENTAL LIMITS ON THE SIZES OF FUNDAMENTAL PARTICLES

To test the finite size of fundamental particles, experiments are performed to search for compositeness, to investigate a non-pointlike behavior or form factors  $R$  in strong, electromagnetic and electroweak interactions. Each interaction is assumed to have its characteristic energy scale related to the characteristic size of interaction region. In the following sub-sections we review the experimental limits on excited particle masses, energy scales and form factors for all three interactions. We elaborate on the new QED results from the L3 experiment performed during 1991 to 1999. The most stringent limits measured from excited states of fermions, non-pointlike couplings and form factors are shown in the left side of the Fig. 1. In the right side they are compared with the Compton wavelengths of FP.

**Strong Interaction** – To test the color charge of the quarks, the entrance channel and the exit channels of the reaction in the scattering experiment should be dominated by the strong interaction. This condition is fulfilled by the CDF  $pp$  data [4] which exclude excited quarks  $q$  with a mass between 80 and 570 GeV at 95% CL. The UA2 data [5] exclude  $u$  and  $d$  quark masses smaller than 288 GeV at 90% CL. In this case characteristic energy scale is given by the mass of the excited quark. Associated characteristic size is  $r_q = h = (m_q c) < 3.5 \cdot 10^{-17}$  cm.

**Electromagnetic Interaction** – In the case of electromagnetic interaction the process  $e^+ e^- \rightarrow (e)$  is ideal to test the QED because it is not interfered by the  $Z^0$  decay [6]. This reaction proceeds via the exchange of a virtual electron in the  $t$ - and  $u$ -channels, while the  $s$ -channel is forbidden due to angular momentum conservation. Total and differential cross-sections for the process  $e^+ e^- \rightarrow (e)$ , are measured at the  $p_T$  energies from 91 GeV to 202 GeV using the data collected with the L3 detector from 1991 to 1999 [1,7{10].

The agreement between the measured cross section and the QED predictions is used to constrain the existence of an excited electron of mass  $m_e$  which replaces the virtual electron in the QED process [11], or to constrain a model with deviation from QED arising from an effective interaction with non-standard  $e^+ e^-$  couplings and  $e^+ e^-$  contact terms [12].

An overall  $t^2$  fit at 95% CL gives for the excited electron  $m_e > 402$  GeV with the QED cut-off parameters  $\tau_+ > 415$  GeV and  $\tau_- > 258$  GeV.  $\tau_+$  and  $\tau_-$  are mass cut-off parameters limiting the existence of a heavy excited electron. In the

case of non-pointlike coupling the cut-off parameter limiting the scale of the interaction is measured to be  $> 1687 \text{ GeV}$ . Characteristic size related to the case of interaction via excited heavy electron is  $r_e = h = (m_e c) < 5 \cdot 10^{-17} \text{ cm}$ . For the case of direct contact term interaction  $r_e = (hc) = 1.17 \cdot 10^{-17} \text{ cm}$ . The behavior of  $r_e^2$  as a function of  $m$  shows no minimum indicating that the size of the interaction region must be smaller than  $r_e$ .

Electroweak Interaction - The ep accelerator HERA and the  $e^+e^-$  accelerator LEP test excited and non-pointlike couplings of quarks and leptons. In the entrance channel the reaction proceeds via magnetic and weak interaction and in the exit channel all three interactions participate.

The H1 data [13] give for the  $q^- q^+$  decay channel a compositeness scale. For a  $q^-$  mass  $100 \text{ GeV}$  the limit on  $m$  moves from  $60 \text{ GeV}$  to  $290 \text{ GeV}$ . In the  $q^- q^+$  decay channel the ep data exclude at  $95\%$  CL large regions of the cross section times branching ratio  $(q^- q^+ \rightarrow B R (q^- q^+))$  for  $q^-$  masses from  $50 \text{ GeV}$  to  $250 \text{ GeV}$ . A similar search has been performed by the ZEUS collaboration [14].

The H1 data [13] describe for the  $e^- e^+$  case the electromagnetic and weak decay channel. For the  $e^- e^+$  channel  $m$  is measured. The experiment is able to set limits on the product  $B R$  of the production cross section and the branching ratio for different decay channels. Big regions of the product  $B R$  in the decay channels of  $e^- e^+, e^- e^+ \rightarrow eZ^0, e^- eW^- \rightarrow \tau^+$  are excluded by the data in the  $e^- e^+$  mass range up to  $250 \text{ GeV}$  at  $95\%$  CL.

At the LEP, excited quarks and leptons could be produced via a  $Z^0$ ; coupling to fermions. The ALEPH investigated the  $q^- q^+ g$  and  $q^- q^+ \gamma$  decay channels and 16 channels from the states  $11, \bar{1}\bar{1}, 1\bar{1}$  and  $\bar{1}\bar{1}$  [15]. No evidence for weak

EXCITED STATE	QCD		QED		EW		FORMFACTOR	
	mass GeV	$\Lambda_+$ GeV	$\Lambda_-$ GeV	mass $10^{18} \text{ cm}$	$\Lambda_+$ TeV	$\Lambda_-$ TeV	size $10^{18} \text{ cm}$	
q	570	-	-	-				
u	288	-	-	-				
d	288	-	-	-				
e	-	415	258	402	50.0			
$\mu$	-	-	-	-	-			
$\tau$	-	-	-	-	-			
f	-	-	-	-	-			
NON POINTLIKE								
q	-	-	-	-	4.4	6.0	4.5 3.3	
u	-	-	-	-	12.9	6.6	1.5 3.0	
d	-	-	-	-	5.7	9.8	3.5 2.0	
e	-	1687	-	11.7	11.1	13.2	1.8 1.5	
$\mu$	-	-	-	-	15.3	7.4	1.3 2.7	
$\tau$	-	-	-	-	10.2	9.5	1.9 2.1	
f	-	-	-	-	16.9	12.5	1.2 1.6	
	-	-	-	-	17.9	11.7	1.1 1.7	
FORMFACTOR	q						28	
	u						-	
	d						29	
	e						21	
	$\mu$						30	
	$\tau$						19	
	f						-	

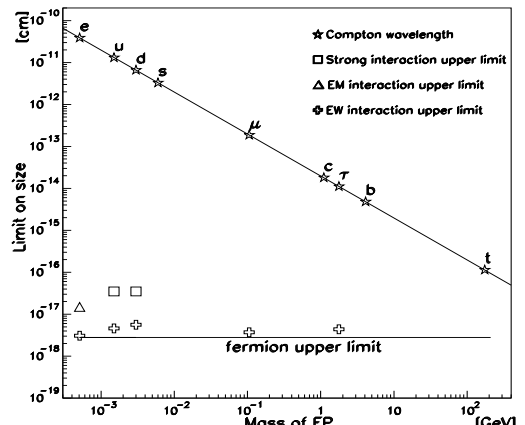


FIGURE 1. In the left side the most stringent experimental limits of FPPs are presented. The right side shows the comparison of Compton wavelengths of FPPs with the current experimental limits measured for strong, electromagnetic and weak interaction.

decay of excited quarks or leptons has been found and stringent coupling limits are set. By combining all radiative channels under investigation a lower limit on the compositeness mass at a scale  $> 16$  TeV for leptons could be established. L3 [16] and OPAL [17] report similar results.

The search for non-pointlike coupling of the quarks and leptons is also performed with  $e^+e^-$  accelerators. The L3 searched at center-of-mass energies between 130 GeV and 172 GeV for new effects involving four fermion vertices contact interactions in all exit channels [18]. In particular the L3 investigated the pure contact interaction amplitudes  $e^+e^- \rightarrow f^+f^-$  and form factors for quark and leptons [18,2].

The most stringent limits for all three interactions are summarized in the left side of the Fig. 1. In the right side of the Fig. 1 a comparison is shown of the Compton wavelength  $\lambda_c$  of FP with current experimental limits measured in strong, electroweak and weak interaction. In conclusion all data show no signal, Fig. 1 demonstrates that  $\lambda_c$  is always bigger than the characteristic size of the interaction area. This experimental fact is used in the next section to estimate the sizes of FP and the mass of a Higgs scalar.

## CHARACTERISTIC SIZES RELATED TO GRAVITY

Selfgravitating particlelike structure with de Sitter vacuum core—De Sitter-Schwarzschild geometry originated from replacing a black hole singularity with de Sitter vacuum core. The idea goes back to the 1965 paper by Gliner who interpreted the Einstein cosmological term  $\Lambda$  as a vacuum stress-energy tensor  $T^{\text{vac}} = (8\pi G)^{-1}g = \Lambda g$  and suggested that it could be a final state in a gravitational collapse [19]. In the 80-s several solutions have been obtained by direct matching de Sitter metric inside to Schwarzschild metric outside of a junction surface [20]. All matched solutions have a jump in a metric at the junction surface, since the O'Brien-Synge junction condition  $T_{\text{nn}} = 0$  is violated there [21]. The exact analytic solution avoiding this problem and representing globally regular de Sitter-Schwarzschild geometry, asymptotically Schwarzschild as  $r \rightarrow 1$  and asymptotically de Sitter as  $r \rightarrow 0$ , was found in the Ref. [22].

The main steps to find this solution are to insert the spherically symmetric metric

$$ds^2 = e^{\phi} dt^2 - e^{\phi} dr^2 - r^2(d\theta^2 + \sin^2\theta d\phi^2) \quad (1)$$

into the Einstein equations  $R - \frac{1}{2}Rg = \frac{8\pi G}{c^4}T$  which then take the form

$$\frac{e}{r^2} + \frac{\phi}{r} + \frac{1}{r^2} = \frac{8\pi G}{c^4}T_t^t; \quad \frac{e}{r^2} - \frac{\phi}{r} + \frac{1}{r^2} = \frac{8\pi G}{c^4}T_r^r \quad (2)$$

$$\frac{1}{2}e \left( \frac{\phi}{2} + \frac{1}{r} + \frac{0}{2} \right) = \frac{8\pi G}{c^4}T = \frac{8\pi G}{c^4}T \quad (3)$$

To match smoothly the de Sitter metric inside to the Schwarzschild metric outside, the boundary conditions are imposed on the stress-energy tensor such that  $T_{\text{nn}} = 0$

as  $r \neq 1$  and  $T \neq -\frac{1}{\rho} \rho$  as  $r \neq 0$ , with  $\rho$  as de Sitter vacuum density at  $r = 0$ . For both de Sitter and Schwarzschild metrics the condition  $T^t_t = T^r_r$  is valid, which defines the class of spherically symmetric solutions with the algebraic structure of the stress-energy tensor  $T$  such that  $T^t_t = T^r_r$  and  $T^r_r = T^t_t$ .

The stress-energy tensor of this structure describes a spherically symmetric vacuum, invariant under the boosts in the radial direction (Lorentz rotations in  $(r; t)$  plane) [22], and can be interpreted as  $r$  dependent cosmological term [23]. It smoothly connects the de Sitter vacuum at the origin with the Minkowski vacuum at infinity and generates the metric

$$ds^2 = 1 - \frac{R_g(r)}{r} dt^2 - 1 - \frac{R_g(r)}{r} dr^2 - r^2(d^2 + \sin^2 d^2) \quad (4)$$

where

$$R_g(r) = \frac{2GM(r)}{c^2}; \quad M(r) = \frac{4}{c^2} \int_0^r T_t^t(r) r^2 dr \quad (5)$$

For any density profile, satisfying the conditions of needed asymptotic behaviour of a metric at the origin and of a finiteness of a mass, this metric describes de Sitter-Schwarzschild geometry, asymptotically Schwarzschild at infinity and asymptotically de Sitter at the origin [24]. In the model of Ref. [22] the density profile  $T_t^t(r) = \rho(r)c^2$  has been chosen as

$$= \rho_{vac} e^{-4\rho_{vac}r^3/3m} = \rho_{vac} e^{-r^3/r_0^2 r_g} \quad (6)$$

which describes, in the semiclassical limit, vacuum polarization in the gravitational field [24]. Here  $r_0^2 = 3c^2/8G$  is the de Sitter horizon,  $r_g = 2Gm/c^2$  is the Schwarzschild horizon, and  $m$  is the gravitational mass of an object.

The metric  $g_{tt} = 1 - \frac{R_g(r)}{r}$  is shown in Fig. 2. The fundamental difference from the Schwarzschild case is that de Sitter-Schwarzschild black hole has two horizons, the black hole horizon  $r_+$  and the internal Cauchy horizon  $r_q$  ( $g_{tt}(r_q) = 0$ ).

The object is a black hole from  $m > m_{cr} = 0.3m_{Pl}$ . It loses its mass via Hawking radiation until a critical mass  $m_{cr}$  is reached where the Hawking temperature drops to zero [24]. At this point the horizons come together. The critical value  $m_{cr}$  puts the lower limit for a black hole mass. Below  $m_{cr}$  de Sitter-Schwarzschild geometry (4) describes a neutral selfgravitating particlelike structure with  $T \neq -\rho$  at the origin [24]. This fact does not depend on particular form of a density profile [24] which must only guarantee the boundary condition at the origin and the finiteness of the mass as measured by a distant observer

$$m = 4 \int_0^r \rho(r) r^2 dr \quad (7)$$

De Sitter-Schwarzschild geometry has two characteristic surfaces at the characteristic scale  $r = (r_0^2 r_g)^{1/3}$  [24]. The first is the surface of zero scalar curvature. The scalar curvature  $R = 8GT$  changes its sign at the surface

$$r = r_s = \frac{m}{\text{vac}}^{1=3} = \frac{1}{1=3} \frac{m}{m_{p1}}^{1=3} \frac{p_1}{\text{vac}}^{1=3} l_{p1} \quad (8)$$

which contains the most of the mass  $m$ . Gravitational size of a selfgravitating particlelike structure can be defined by the radius  $r_s$ . The second surface is related to the strong energy condition of the singularity theorem  $s$ ,  $(T - g)T = 2u \cdot u \geq 0$ , where  $u$  is any timelike vector. It is violated at the surface of zero gravity

$$r = r_c = \frac{m}{2 \text{vac}}^{1=3} = \frac{1}{(2)^{1=3}} \frac{m}{m_{p1}}^{1=3} \frac{p_1}{\text{vac}}^{1=3} l_{p1} \quad (9)$$

Both these characteristic sizes represent modification of the Schwarzschild gravitational radius  $r_g$  to the case of a finite density  $\text{vac}$  at the origin.

Sizes of lepton vacuum cores and an upper limit on a scalar mass  $m$ .  
de Sitter-Schwarzschild particlelike structure cannot be applied straightforwardly to approximate a structure of a FP like an electron which is much more complicated. However, in the frame of our assumption a mass of a FP is related to its gravitationally induced core with de Sitter vacuum  $\text{vac}$  at  $r = 0$ . This allows us to estimate the minimum geometrical size of a FP defined by de Sitter-Schwarzschild geometry as a size of its vacuum core  $r_c$ , if we know  $\text{vac}$  and  $m$ .

In the context of spontaneous symmetry breaking the vacuum density  $\text{vac}$  is related to the vacuum expectation value  $v$  of a Higgs field which gives particle a mass  $m_p = gv$ , where  $g$  is the relevant coupling to the scalar. For a Higgs particle  $g = 2$ , where  $2$  is its self-coupling. It is neutral and spinless, and we can approximate it by de Sitter-Schwarzschild particlelike structure, identifying  $\text{vac}$  with the self-interaction of the Higgs scalar in the standard theory

$$\text{vac} = v^4 = 4 \quad (10)$$

We assume also that the gravitational size of a particle  $r_s$  is restricted by its Compton wavelength,  $r_s \ll c$ . This assumption is suggested by all experimental data about limits on the sizes of FP. This gives

$$\frac{r_s}{c} = \frac{16}{1} ; \quad \frac{1}{16} \quad (11)$$

With this limit on a self-coupling we estimate an upper limit on a Higgs scalar mass at the electroweak scale ( $v = 246$  GeV) by

$$m_{\text{scalar}} = 154 \text{ GeV} \quad (12)$$

For a lepton getting its mass from the electroweak scale, its inner core is determined by this scale. Putting Eq.(10) into the Eq.(9) we get for a size of a vacuum core of a lepton with the mass  $m_1$

$$r_c = \frac{2m_1}{v^4}^{1=3} \quad (13)$$

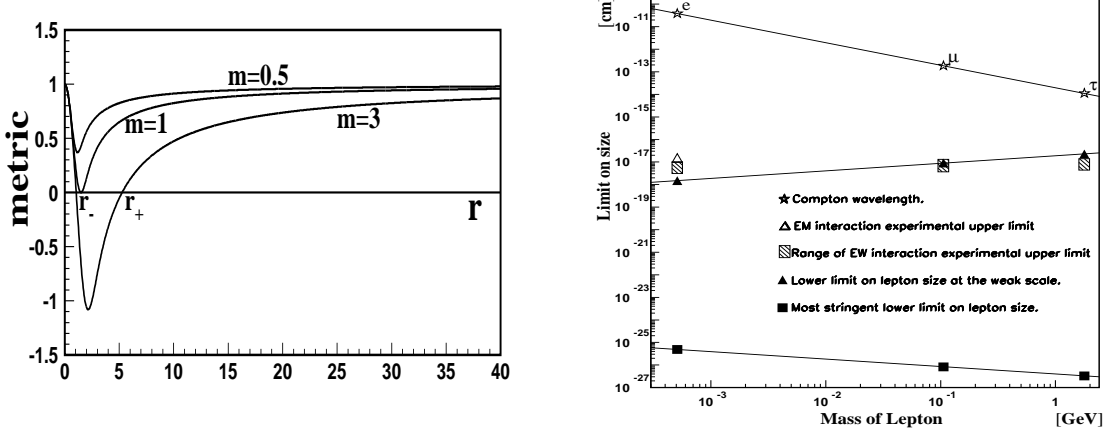


FIGURE 2. In the left side vacuum configurations described by de Sitter-Schwarzschild geometry (4)  $g_{tt} = 1 - R_g(r)/r$  are presented. The mass  $m$  is normalized here to  $m_{cr}$ . The case  $m > 1$  represents a black hole,  $m = 1$  its extreme state, and  $m < 1$  a selfgravitating particlelike structure with de Sitter vacuum core. The right side shows the Compton wavelength of leptons as compared with experimental limits of electromagnetic and weak interaction, and estimated lower limits for the sizes of leptons.

Then the constraint on (11) sets the lower limits for the sizes of lepton vacuum cores by  $r_c^{(e)} > 1.5 \cdot 10^{-18} \text{ cm}$ ,  $r_c^{(\mu)} > 0.9 \cdot 10^{-17} \text{ cm}$ , and  $r_c^{(\tau)} > 2.3 \cdot 10^{-17} \text{ cm}$ .

To estimate the most stringent limit on  $r_{vac}$  we take into account that quantum region of localization  $c$  must within a causally connected region bounded by the de Sitter horizon  $r_0$ . The requirement  $c < r_0$  gives the limiting scale for a vacuum density  $\rho_{vac}$  related to a given mass  $m$

$$r_{vac} \leq \frac{3}{8} \frac{m}{m_{Pl}}^{1/2} \quad (14)$$

This condition connects a mass  $m$  with the scale for  $\rho_{vac}$  at which this mass could be generated in principle, whichever would be a mechanism for its generation.

In this case we get from the Eq.(9) the most stringent, model-independent lower limit for a size of vacuum core

$$r_c > \frac{4}{3}^{1/3} \frac{m_{Pl}}{m_1}^{1/3} \quad (15)$$

Inserting the masses of the leptons  $m_1$  into Eq.(15), we find  $r_c^{(e)} > 4.9 \cdot 10^{-26} \text{ cm}$ ,  $r_c^{(\mu)} > 8.3 \cdot 10^{-27} \text{ cm}$ , and  $r_c^{(\tau)} > 3.3 \cdot 10^{-27} \text{ cm}$ .

For a scalar we put Eq.(10) and  $m_{scalar} = \frac{2}{3} v$  into Eq.(14) and get the limit on the vacuum expectation value  $v = 3 = m_{Pl}$  valid for any self-coupling. The

restriction Eq.(11) gives an upper  $\lim_{q \rightarrow \infty}$  for a scalar mass scalar  $m_{\phi} \approx 3=8m_P$ . These numbers give model-independent constraints for the case of particle production in the course of phase transitions in the very early universe.

The limits on the sizes of FP are summarized in Fig 2, compared to the  $\gamma_c$  and to current experimental limits. The important is that the most stringent limits on sizes of FP as estimated in the frame of de Sitter-Schwarzschild geometry, are much bigger than the Planck length  $l_P = 10^{-33}$  cm, what justifies our approach.

#### ACKNOWLEDGEMENTS

We are grateful to Samuel C. C. Ting for his strong support of this project, and to Martin Pohl for stimulating discussions of this paper.

#### REFERENCES

1. L3 Collaboration, Acciarri, M., et al., Phys. Lett. B 384, 323 (1996).
2. Bourilkov, D., Phys. Rev. D 62, 076005 (2000).
3. Dymnikova, I., Ulbricht, J., and Zhao, J., Grav. & Cosm. 6, 1 (2000).
4. CDF Collaboration, Abe, F., et al., Phys. Rev. D 55, R5263 (1997).
5. UA2 Collaboration, Alitti, J., et al., Nucl. Phys. B 400, 3 (1993).
6. Bajc, A., Dymnikova, I., Sakharov, A., Sanchez, E., Ulbricht, J., and Zhao, J., this volume.
7. Wu, J., Ph.D. thesis, Chinese University of Science and Technology, USTC (1997).
8. Roth, B., Ph.D. thesis, RWTH Aachen (1998).
9. L3 Collab., Acciarri, M., et al., Phys. Lett. B 413, 159 (1997).
10. L3 Collab., Acciarri, M., et al., Phys. Lett. B 475, 189 (2000).
11. Little, A. M., Ph.D. thesis Harvard University, (1970).
12. Eboli, O. J. P., Phys. Lett. B 271, 274 (1991).
13. H1 Collaboration, Adloff, C., et al., Nucl. Phys. B 483, 44 (1997).
14. ZEUS Collaboration, Derrick, M., et al., Z. Phys. C 65, 627 (1995).
15. ALEPH Collaboration, Barate, R., et al., Preprint CERN/EP/98-022 (1998).
16. L3 Collaboration, Michael, J., et al., Proceedings of the 29th International Conference on High Energy Physics, Vancouver, Canada, 1998, edited by Alan Astbury, World Scientific, Singapore (1999).
17. OPAL Collaboration, Akrawy, M. Z., et al., Phys. Lett. B 246, 285 (1990).
18. L3 Collaboration, Acciarri, M., et al., Phys. Lett. B 433, 163 (1998).
19. Gliner, E. B., Sov. Phys. JETP 22, 378 (1966).
20. Bernstein, M. R., Bull. Amer. Phys. Soc. 16, 1016 (1984); Fahri, E., and Guth, A., Phys. Lett. B 183, 149 (1987); Shen, W., and Zhu, S., Phys. Lett. A 126, 229 (1988); Frolov, V. P., Markov, M. A., and Mukhanov, V. F., Phys. Rev. D 41, 3831 (1990).
21. Poisson, E., and Israel, E., Class. Quant. Grav. 5, L201 (1988).
22. Dymnikova, I., Gen. Rel. Grav. 24, 235 (1992).
23. Dymnikova, I. G., Phys. Lett. B 472, 33 (2000).
24. Dymnikova, I. G., Int. J. Mod. Phys. D 5, 529 (1996).